Journal of Rock Mechanics & Tunnelling Technology (JRMTT)
20 (1) 2014 pp 5-20

Available online at www.isrmtt.com

The Behaviour of Rock Support in Tunnels in Seismic Regions with a Case Study of a Large Underground Cavern in the Himalayas

Rajinder Bhasin, Thomas Pabst*

Norwegian Geotechnical Institute, Norway

**Corresponding author: rkb@ngi.no*

ABSTRACT

Underground structures can be adversely affected during earthquake events. Several cases have been reported internationally on damages to underground structures during major earthquakes. This paper reviews and provides some important insights into the behaviour of rock support in tunnels under the effect of earthquake loading. Numerical experiments have shown that for a continuum weak rock mass the maximum axial force on the tunnel lining increases significantly when dynamic loading is applied as compared to static loading. For competent and hard rock masses the increase in maximum axial force on the lining is insignificant when dynamic loading is applied. In addition, for a weak rock mass subjected to earthquake loading, the forces on a tunnel lining increases significantly when the dimension of an opening is increased as compared to a competent rock mass.

A case study on the stability of a large underground cavern with earthquake loading is illustrated. The cavern, which constitutes a major component of Hydro Power Project, is experiencing a number of instabilities. Approximately 5 percent of the bolts in the powerhouse are reported to have failed and the walls of the cavern are continuing to converge, albeit at a slow rate since its completion (3-6 mm per year). Plans are underway to stabilize this important underground structure. Numerical simulations have been performed to help better understand the behaviour of a rock mass surrounding the cavern. The results from the analysis indicate that possibly there was an underestimation of the rock support requirements needed for the cavern. Based on these simulations, it also seems that in the present conditions an earthquake could lead to large displacements and instabilities.

Keywords: Tunnel; Numerical analysis; Cavern; Earthquake; Rock mass

1. INTRODUCTION

Some underground structures have undergone severe damages during recent large earthquakes such as 1995 Kobe, Japan, the 1999 Chi-Chi, Taiwan, the 1999 Kocaeli, Turkey and the 2008 Wenchen (Tibet-China) (Bhasin et al, 2006; Aydan et al, 2010). Research studies in this field, which were mainly initiated by such evidences, showed that the impact of earthquakes on tunnel lining can be significant, especially in weaker rocks.

The behaviour of a tunnel is sometimes approximated to that of an elastic beam subject to deformations imposed by the surrounding ground. Three types of deformations (Owen and Scholl, 1981) express the response of underground structures to seismic conditions (see Fig. 1):

(i) axial compression and extension
(ii) longitudinal bending
(iii) ovaling/racking

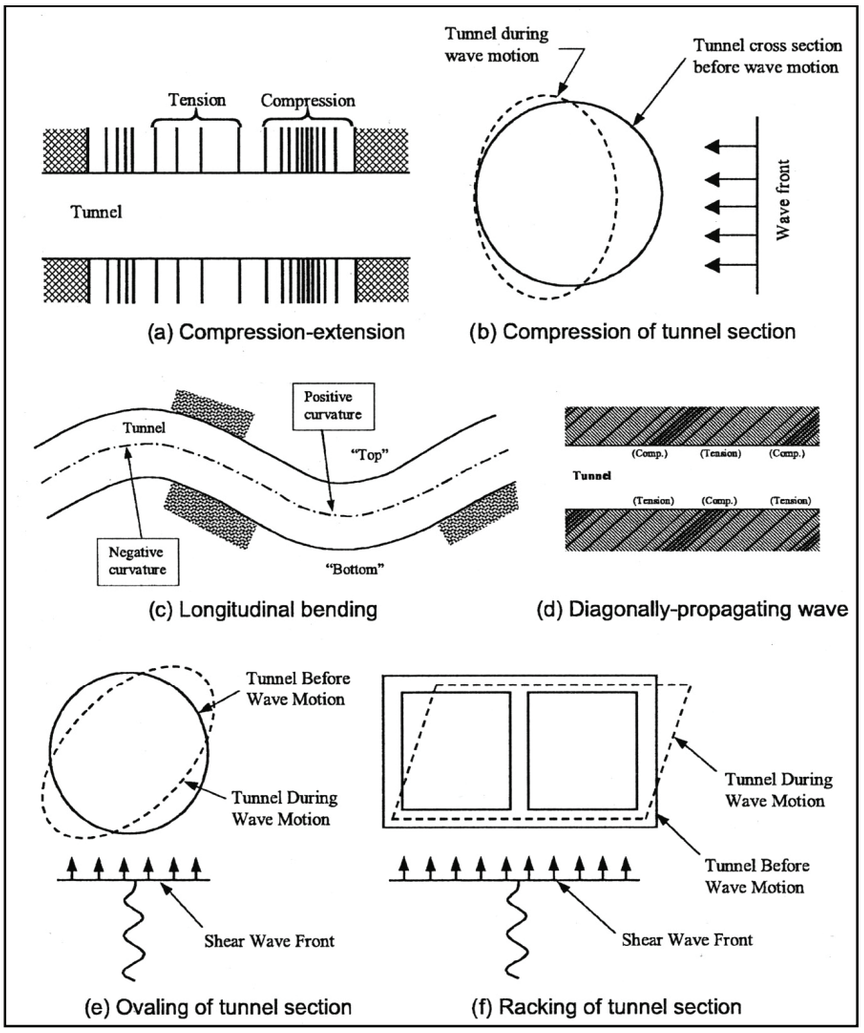

Fig. 1 - Deformation modes of tunnels due to seismic waves (after Owen and Scholl, 1981)

Axial deformations in tunnels are generated by the components of seismic waves that produce motions parallel to the axis of the tunnel and cause alternating compression and tension. Bending deformations are caused by the components of seismic waves producing particle motions perpendicular to the longitudinal axis. Design considerations for axial and bending deformations are generally in the direction along the tunnel axis (Wang, 1993). Ovaling or racking deformations in a tunnel structure develop when shear waves propagate normal or nearly normal to the tunnel axis, resulting in a distortion of the cross-sectional shape of the tunnel lining.

2. NUMERICAL ANALYSES OF TUNNEL LININGS

A series of numerical simulations using a Finite Element Code (FEM) were performed to investigate the effect of seismicity on tunnel lining in tunnels of different sizes (Bhasin et al., 2006). Both linearly elastic (competent rock) and elastic-plastic (weak rock) analyses were performed with rock support interaction. Subsequently in the simulations, joints were also introduced in the body of the models to study the effect of seismicity on tunnels in jointed rock mass.

It may be noted that in the continuum elastic analysis the material surrounding the excavation cannot undergo progressive failure such as in poor rock masses. In the plastic case, the material is defined as elastic-perfectly plastic in which no brittle failure can occur.

In all the numerical models the horizontal and vertical lateral boundaries for each of the tunnel sizes is more than 3 times the diameter of the excavation from the roof of the opening. The overburden above the tunnel roof for each of the tunnel sizes (varying from 5 to 20 m in diameter) was kept constant so that the initial in-situ stress was the same before the excavation of the tunnel.

After excavation of tunnel in each of the different tunnel models, a full lining in the form of a 10 cm thick shotcrete was applied. Then a seismic loading was applied and the models were then run to equilibrium for both the elastic and plastic cases till the maximum axial force along the periphery on the tunnel lining was obtained.

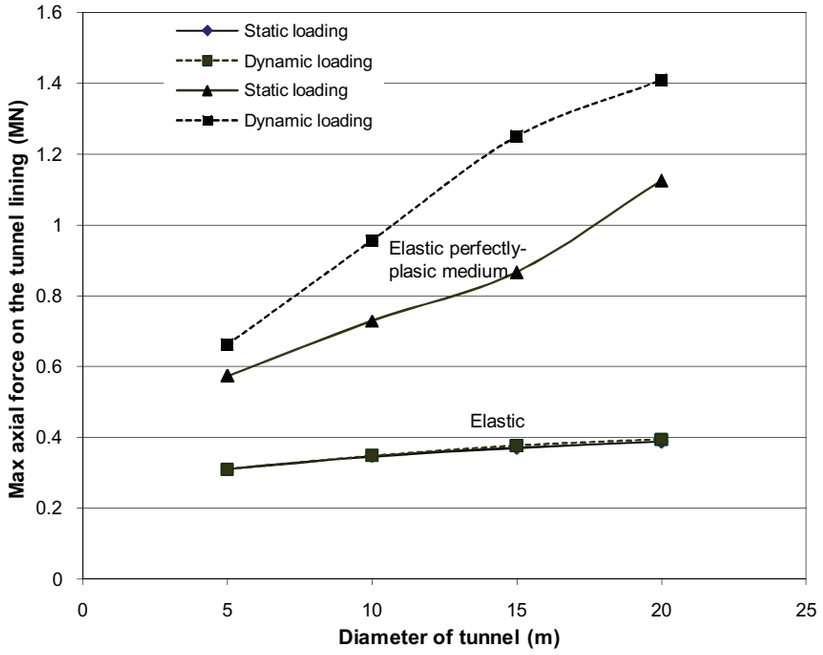

Fig. 2 - Summary of numerical results for tunnels of different sizes

Elastic and plastic analysis studies were performed for tunnels of different sizes and the results are summarised in Figure 2 (Bhasin et al, 2006). It can be seen from this figure that for the elastic analysis there is not much difference in the maximum axial force on the lining as the tunnel dimension increases from 5 to 20 m. In addition, there is not much difference in the maximum axial force on the lining when dynamic loading is applied as compared to static loading. For plastic analysis the load on the lining increases significantly with the tunnel diameter. This is in line with the studies carried out by Bhasin and Grimstad (1996) and the observations of Singh et al, (1992)

which showed that the rock support pressure in tunnels in weak rocks is dependent on the dimensions of the tunnel. These numerical simulations show, that in weak rocks, there is a significant increase in the maximum axial force when dynamic loading is applied as compared to static loading.

The above analysis indicated that, from the cases studied, in an elastic (homogenous rock mass) medium the underground structure is less sensitive to seismic effects than for an elastic-perfectly plastic medium. For the elastic-perfectly plastic (weak rock mass) medium the difference in the axial force on the lining between the static and dynamic loading ranges from about 15% to 44%. This means that for a weak rock mass the support capacity of the lining should be increased to withstand the effect of seismicity.

3. EFFECT OF SEISMICITY ON TUNNELS IN ROCK WITH JOINTS

The effect of discontinuities in the models was investigated using identical loads and material configurations as in the earlier models (Bhasin et al., 2010). A single horizontal and vertical joint and multiple parallel joints around the excavations were investigated. The joints were described by Mohr-Coulomb slip criterion. Neither groundwater pore pressure nor any additional pressures were added to the joints. Figure 3 shows that, in competent rock, for all the loading conditions the maximum axial force on the lining occurs at the intersection between the joint and the tunnel lining. Please note that h and v are the seismic coefficients in the horizontal and vertical directions respectively. The seismic coefficients are dimensionless coefficients which represent the (maximum) earthquake acceleration as a fraction of the acceleration due to gravity. Typical values are in the range of 0.1 to 0.3. The seismic force in the model is applied as an additional Body Force to each element, and is vectorially added to the downward Body Force which exists due to gravity. Joints act as wave-guides accentuating damage to the tunnel support.

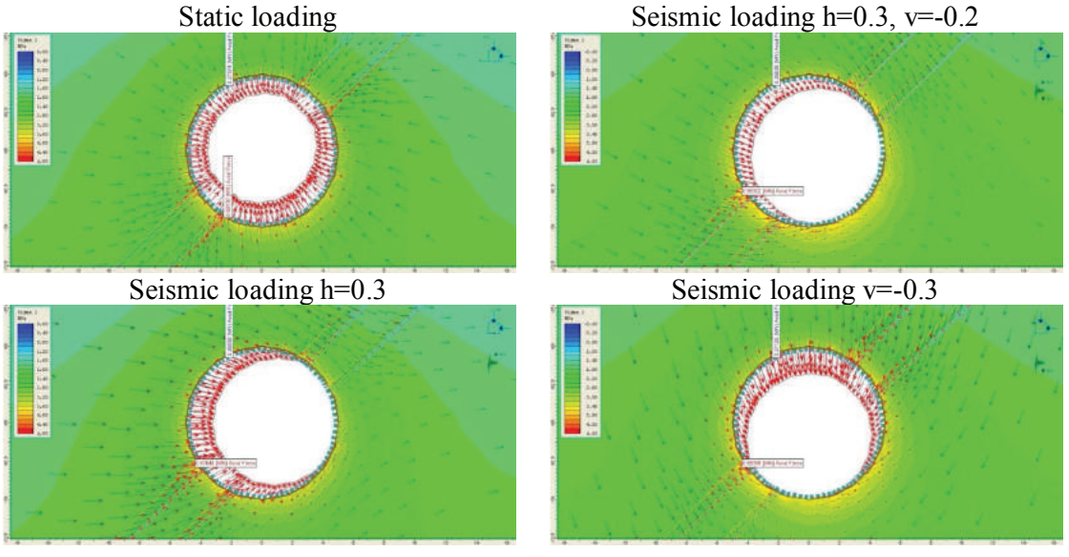

Fig. 3 - Effect of two parallel joints in competent rock (h and v are the seismic coefficients in the horizontal and vertical directions)

For weak rock masses, the maximum axial force on the lining did not always occur at the intersection between the joint and lining (see Fig. 4). This may be due to the fact that weak rocks are able to deform independent of joints. More details on wave-guide action of parallel joints can be found in Heuze and Morris (2007) and Bhasin et al. (2010).

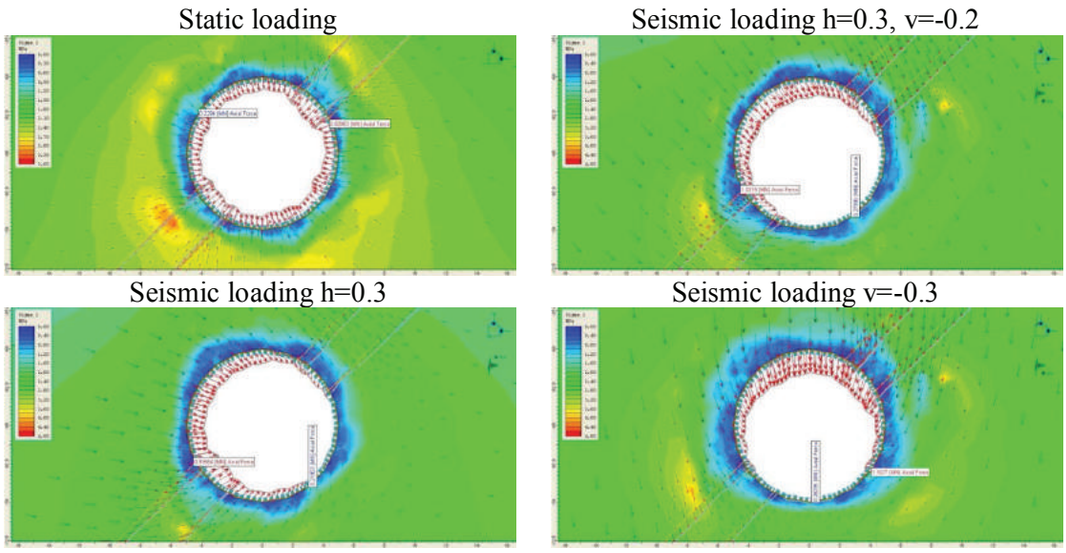

Fig. 4 - Effect of two parallel joints in weak rock (h and v are defined in Fig. 3)

4. TUNNEL SUPPORT STRATEGY IN SEISMIC REGIONS

Barton (1984) advocated the use of simple rule of thumb to select appropriate rock reinforcement for underground structures in seismic regions. Based on the Q-system of rock mass classification (Barton et al, 1974) it was suggested that the rock mass quality number 'Q' in seismic regions may be assumed as half compared to Q-static i.e.:

$$Q_{seismic} \approx \tfrac{1}{2}\ \mathrm{Q}_{\mathrm{static}} \approx \frac{RQD}{J_n} \times \frac{J_r}{J_a} \times \frac{J_w}{2.SRF} \qquad (1)$$

The 50 % reduction of Q(static) obtained by assuming 2.SRF (equation 1) actually gives a 25% increase in support pressure, due to the gradient of the slope in Figure 5. This 25 % increase is surprisingly in the range of 15-44% increase in maximum axial force that was observed for seismic conditions through numerical modelling studies. Hence, the above tunnel support strategy agrees well with the numerical studies carried out. It is however, important to add that the use of rock mass reinforcement and tunnel support method such as the Q-system will not be appropriate in cases where adverse geological features such as wedges or faults exists. Such cases warrant special design of reinforcement based on the orientation and strength-deformation properties of the geological features (Barton, 1984 & 1994).

In the Q-system support design chart (Fig. 6), a substantial amount of data was analysed and recommendations for supporting poor rock masses using reinforced ribs of sprayed concrete (RRS) as a function of the load from the rock were given. The analytically calculated loads (= support pressure) linked to rock mass qualities were compared with practical rock support practices in Norwegian tunnels. Based on this the recommended design of RRS with thickness, number of rebars and the spacing between each RRS was given in the support chart shown in Figure 6.

5. CASE STUDY ON THE STABILITY OF A LARGE UNDERGROUND CAVRN IN THE HIMALAYAS

Several large hydroelectric power plants have been built in the Himalayas over the past few years (see Goel et al., 2012). Tala hydroelectric project is currently the biggest operating hydro power project in Bhutan (Singh et al., 2007). This 1020 MW hydroelectric project is a joint project between India and Bhutan generating 4865 GWh/yr. It is located on the Wangchu River, in the Western part of the country. In this paper focus is placed on its machine hall, in which large instabilities have been experienced.

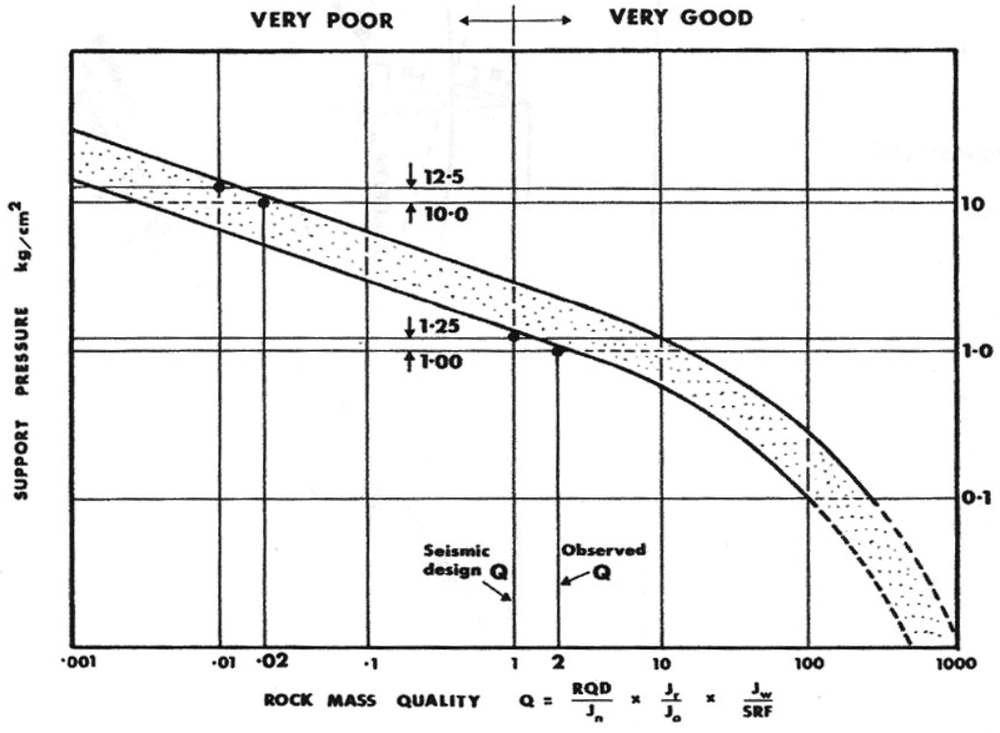

Fig. 5 - Seismic reduction of Q-value to obtain 25% increase in support pressure (Barton, 1984)

The geological formations at the powerhouse area consist of highly deformed and tightly folded bedded sequences of quartzite and amphibolites schist partings. The rock mass rating (RMR) varies from 19 to 50 and the rock mass quality Q ranges from 0.11 to 14 (very poor to good).

The powerhouse is located close to a major thrust zone called MCT (Main Central Thrust) which is marking the boundary between the Lesser and Higher Himalayas. It is a major tectonic feature and the single largest structure within the Indian plate that has accommodated Indian-Asian convergence. Although no conclusive link has been established between this thrust feature and the instability experienced in powerhouse cavern, this feature is of concern for the long-term stability of the cavern (especially regarding local seismic activity; Naik et al., 2011b; Bhasin et al., 2013).

The cavern itself is about 200 m long, 45 m high and 20 m wide (Figure 7, Naik et al., 2011b). The National Institute of Rock Mechanics (NIRM) in India had carried out the in-situ stress measurements by the hydrofracture method and these were estimated as - vertical stress σ_v = 10.9 MPa (approximately 400 m rock overburden) and minimum horizontal stress σ_h = 9.5 MPA (approximately normal to the cavern axis) and maximum horizontal stress

σ_H = 14.2 MPa (approximately parallel to the cavern axis). The unconfined compressive strength of the intact rock was reported to be about 63 MPa.

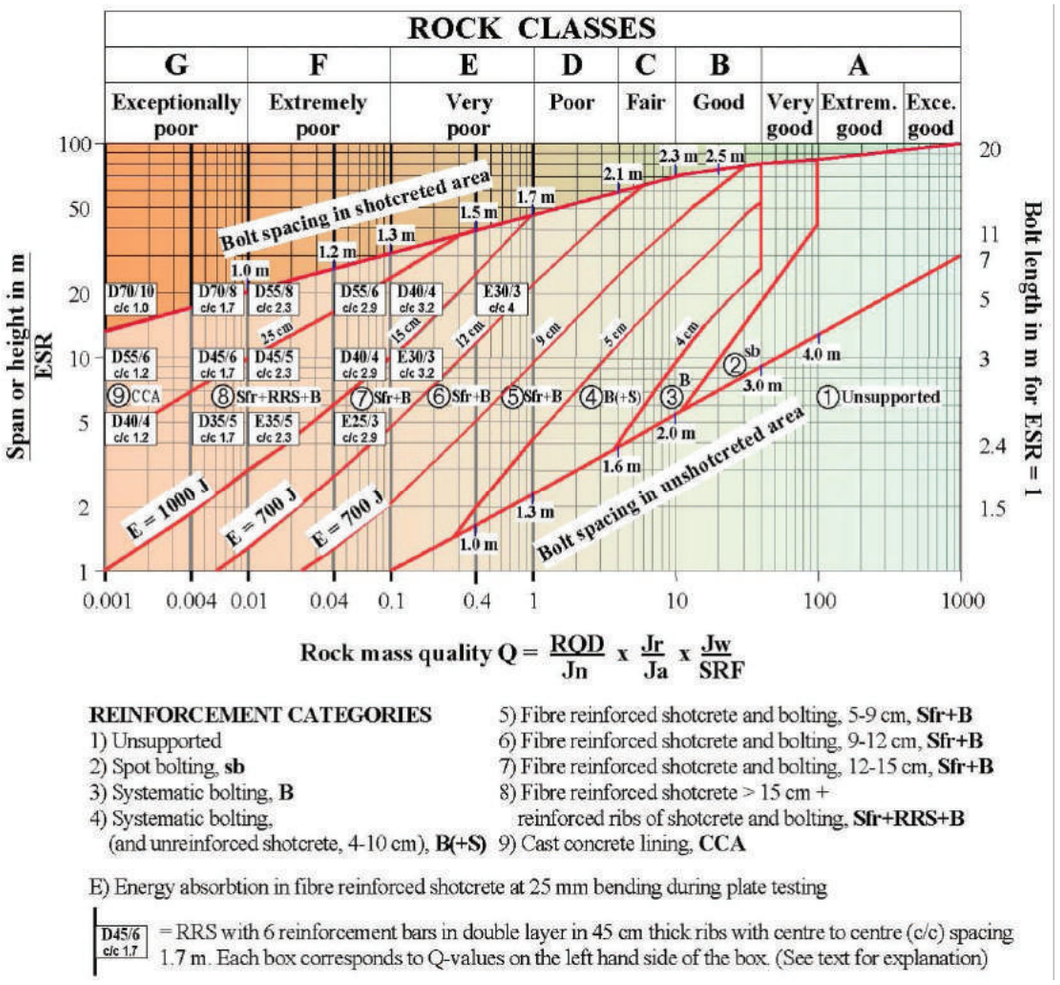

Fig. 6 - Updated Q-system support chart (Grimstad et al., 2003)

The rock support system consists of 26.5 mm diameter and 12 m long fully grouted tensioned Dywidag bolts, plus 150 mm thick shotcrete (Sharma et al., 2004). The yield strength of the bolts was 1033 N/mm^2 (i.e. 571 KN for 26.5 mm diameter rock bolts) and the percentage elongation was 8% (WAPCOS, 2011). The rock bolts were installed at a spacing of 1.5m c/c within the rows and also between the rows (staggered rows).

Total station measurements have monitored large convergence: up to 300 mm during the construction and up to 60 mm during the post construction phase (e.g. Sripad et al., 2003). At the same time, a large number of bolts have started to fail from early 2003 (190, that are 4% of all the installed bolts, in April 2011; Naik et al., 2011a). Most of the failed bolts (147) are from the upstream wall of the cavern. When these rock bolts break they produce a high decibel sound and at times come out of the holes. The length of broken portion of rock bolts varied from a few centimetres to a few meters. This has caused concerns to the project authorities because there are possibilities that those broken portions of the rock bolts may hit the persons working nearby or may hit the electrical panels leading to break down of the generator-turbine set. In addition, it may also lead to instability of the cavern walls. Yet, the situation may be even worse than what has been

reported, since failure of a fully grouted rock bolt is not always visible since it does not necessarily come out of the hole. In addition to bolts failure, shotcrete on the cavern walls is also fractured in some places.

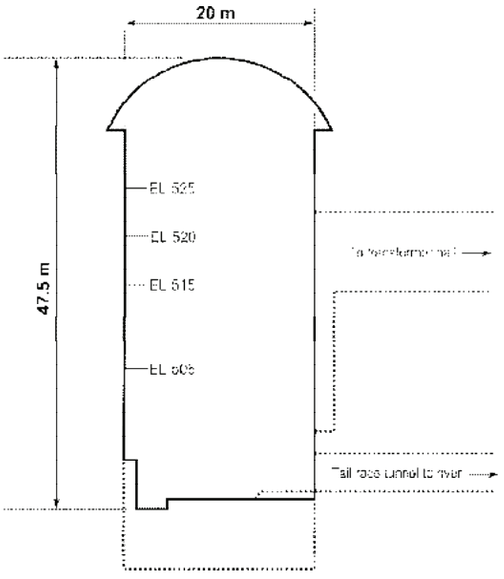

Fig. 7 - Cross section of the machine hall cavern. Elevations are given in meters. Dashed lines indicate access roads and sump trace (not simulated)

Moreover, displacements are still going on, at a rate of about 3 to 6 mm per year. This movement may be due to the deformations occurring along the joint planes in the rock mass thereby increasing the load on the rock bolts. The dynamic movement of the rock mass due to the presence of MCT cannot be ruled out. Hence, for long term stability, the strengthening of the walls of the powerhouse is warranted. But if the convergence of upstream and downstream walls is still continuing, this means also that the load on the rock bolts is still increasing due to the movement of the rock mass surrounding it. And as a matter of fact, during a field visit, in November 2011, it was observed that new rock bolts had been partially shot out of the holes (extruded sections varying from a few centimetres to more than one meter). Measures are being taken to prevent further instability and additional support or rehabilitation of the existing one is being studied.

The objective of this case study is to use numerical models to simulate what was observed in the machine hall (back analysis) and to use the results to better understand the rock mass and the support behaviour. Earthquake effects on stability are also simulated. The results could also provide some information on how to prevent further bolts failure and improve general support.

6. NUMERICAL SIMULATIONS AND INPUT PARAMETERS FOR CAVERN STUDY

Numerical simulations were carried out to better understand the overall behaviour of the rock mass surrounding the machine hall, and possibly explain the reasons why some bolts failed. Once verified and calibrated, numerical models may also be used to give recommendations to prevent further instabilities and assess the effects of earthquakes on the cavern. The total length of the machine hall is more than 200 m and it is assumed that a 2D-model can represent precisely enough the general behaviour. However, this result is a simplification of the reality, because there are actually some differences in the convergences measured along the machine hall (e.g. Singh, 2005).

In this study, the distinct element code UDEC (Universal Distinct Element Code, v. 5.00, Itasca) was used. The distinct element model has been successfully used to simulate blocky rock structures where mechanical discontinuities control the overall deformation (e.g. Bhasin and Høeg, 1997, 1998). The rock mass is simulated as a group of deformable blocks and the joint properties in the model control how the blocks interact together. In addition to these models, fieite element analysis (FEM) was also used to help calibrate some properties (results not presented here, see Bhasin and Pabst, 2013).

Singh et al. (2002) have reported the major discontinuities in the machine hall cavern. A total of five joint sets (plus the foliation) have been observed. In general, the rock mass is considered as "moderately jointed", which, according to Palmström (1995), corresponds to a volumetric joint count of 3 to 10 joints per cubic meter, resulting in blocks of approximately 0.03 to 1 m^3. Similar observations have been made around the desilting chamber (not simulated here; Rao et al., 2007). The models used in this study are approximately 170 m wide and 200 m high, to prevent any side effects. This means that it was not realistic to simulate all the joints with their actual spacing, otherwise the model would have been too large. Moreover, the continuity of the joints was ensured only on a few meters and orientation and spacing vary a lot (Singh et al., 2002), making it difficult to reproduce exactly what was observed in the cavern. Consequently, it was decided to simulate only four main joint sets. Four zones were defined around the cavern. In the first one (5 m around the cavern), joints spacing was set at 2 m (resulting in a moderately jointed area). The next zones, 10, 20 and 75 m around the cavern, had respectively 4, 8 and 20 m joints spacing. The maximum mesh size is 10 m. Figure 8 presents the model, showing the joint configuration (orientation and spacing) and the mesh.

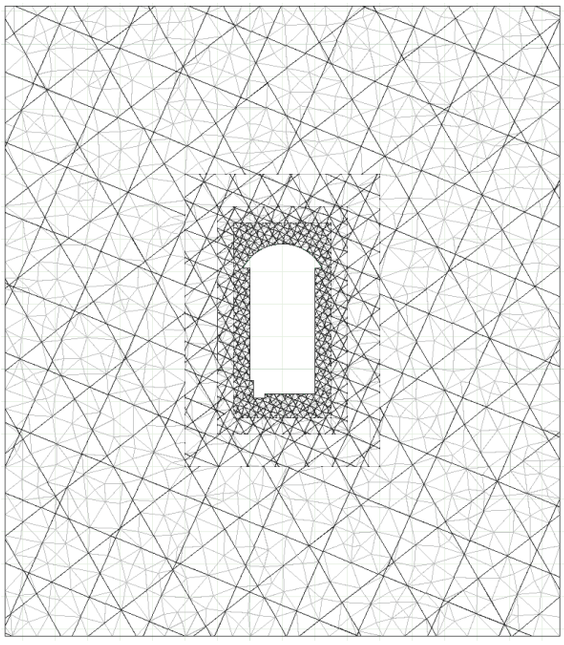

Fig. 8 - Model of the machine hall cavern. Four zones with various joints spacing are simulated (dark lines). Mesh is also shown (grey lines)

Rock mass and joints properties were obtained from the numerous articles published since 2003 for the project (e.g. Singh and Goyal, 2005). Table 1 shows the main parameters input in the numerical models. Rock and joints characteristics, together with stresses, have been measured at the

beginning of the project and used in the models. Mohr-Coulomb failure criterion has been chosen here to simulate both the intact rock mass and the joints (based on numerical simulations carried out by Rao et al. (2003a & 2003b). Remaining uncertainties (e.g. joints sets configurations, lengths of joints or relaxation amplitude) were partly overcome by calibration of the models, based on convergence measured at elevations 506, 515, 520 and 525 (see Fig. 7 for locations).

Relaxation has been simulated: after the excavation has been modeled, approximately 10 cm of deformation has been permitted before the support was installed. That allows the model to reproduce more precisely the real in-situ behaviour.

The support itself consists of cables and liner. The cables are 12 m long and are installed all along the walls (1.5m c/c) and the crown (1.25m c/c). They are pre-tensioned (120 kN) and their yield strength is 1033 N/mm^2 (i.e. 571 kN for 26.5 mm diameter). The liner's main purpose in the simulation is to retain the very small blocks along the cavern walls. Basic default properties were chosen to simulate it. The anchors and the liner are connected.

Table 1 - Input data used in the numerical simulations

Rock mass properties (Sengupta et al., 2007)	
Density	2650 kg/m^3
Young's modulus	6.5 GPa
Poisson's ratio	0.355
Cohesion	2.16 MPa
Friction angle	43°
Field stresses (Sengupta et al., 2007)	
σ_1	10 MPa
σ_2	10 MPa
σ_z	15 MPa
Joints properties (Rao et al., 2003a)	
Shear stiffness JK_s	10 GPa/m
Normal stiffness JK_n	0.97 GPa/m
Cohesion	0.0 MPa
Friction	25°

The sequence of the simulation is as follows. First the model is run and solved without any excavation, to let the model stabilize. The cavern is then excavated, and relaxation happens (maximum 10 cm of displacement). Finally, the support is installed and the calculation is carried out until near-equilibrium (100,000 cycles). Dynamic conditions (earthquake effect) are applied from this last state.

Due to the limited number of data available and the complexity of the system, the goal of the simulations is only to catch the general behaviour of the rock mass and bolt failures.

7. STABILITY RESULTS OF CAVERN

Convergence measurements in the cavern hall (Singh, 2005; Sripad et al., 2003) were compared to displacements simulated by UDEC (Fig. 9). Multiple convergence measurements were taken for each elevation at different locations along the cavern. The range of values obtained is shown in Figure 9. Only two sets of values were available (no continuous monitoring). One obtained after

150 to 250 days (Sripad et al., 2003; dotted lines in Fig. 9) and a second one measured after 500 to 770 days (Singh, 2005; dashed lines in Fig. 9).

Figure 9 shows that the simulation results of the displacements are rather close to the experimental measurements. Note that the "time" or number of cycles simulated is essentially numerical time and does not correlate directly to real time; consequently, "time" dependent results are presented mainly to show a trend and indicate how the displacements tend to stabilize. Moreover, only two measurements of displacement were realized in situ, not enough to properly calibrate a time dependent model. However, this indicates that the model was able to reproduce fairly well the field observations. The final value of convergence simulated is generally slightly lower than measured, showing that the models tend to underestimate somehow the convergence. The differences remain however limited. It may also be due to the fact that after 100,000 cycles, the model is not completely stabilized yet (though not very far from being, considering the asymptotic aspect of the curve). The simulations also show that the displacement is fairly homogenous along the wall, and seems independent of the elevation (punctual measurements in situ are however too scarce to confirm this in the cavern, though the measured values are not that different either).

The displacement is larger on the upstream (right) side of the cavern in the simulations, which confirms field measurements (more bolts have failed along the upstream wall; Naik et al., 2001a). Note however that the transformer hall was not simulated, while it could buffer the stress applied on the upstream part of the machine hall, so the in-situ situation could be worse than predicted here.

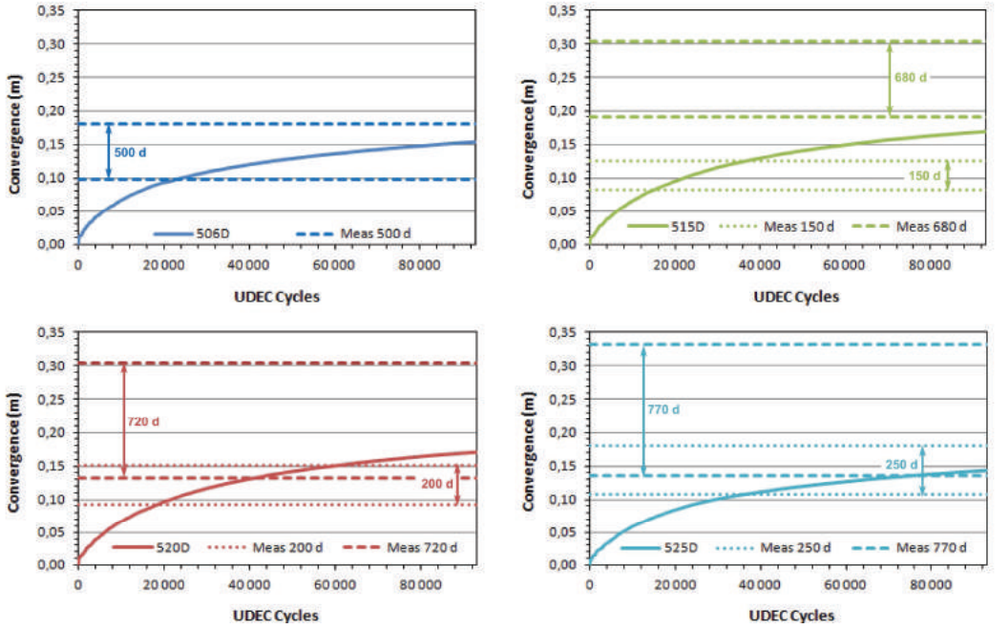

Fig. 9 - Comparison between convergence measurements (dashed lines; maximum and minimum convergence measured at one or two dates, at different positions along the tunnel) and simulated movements (solid line) for different elevations in the cavern ("time" in the models is expressed as calculation cycles, see text for details).

Figure 10 (left) shows maximum total displacements in the cavern. The total maximum displacement is around 15 cm and occurs in the crown. Displacements in the crown and along the walls are rather close and almost the entire cavern seems to endure more than 10 cm of displacement.

In the simulations, bolts that fail on the upstream and downstream walls, are much more numerous than the 4% observed in the cavern (Naik et al., 2011a). However, previous 3D simulations (Naik et al., 2011b) have shown that the proportion of failed bolts could actually be around 25% on each face. The difference may also be due to the difficulty to simulate correctly the bolt action without more precise information about them (e.g. steel and grouting properties) and proper calibration.

Reports dealing with the stability of the cavern have put forth the hypothesis that failure and high convergence may be due to bolts failures, because of bad grouting quality. Another reason, according to the simulation results, could be that the bolts may not be long enough to encompass all the area affected by the excavation. According to the simulation, open joints can reach to a distance of around 20 m from the cavern walls (Fig. 10 right). Note that 20 m is also the recommended distance the bolts should reach to assure stability (because of the possible presence of a weakness zone). The extensometer and convergence measurements show indeed that about 80% of the total deformation occurs in the first 20 m from the wall; this may be a additional indication that the models actually catch rather well the behaviour of the cavern.

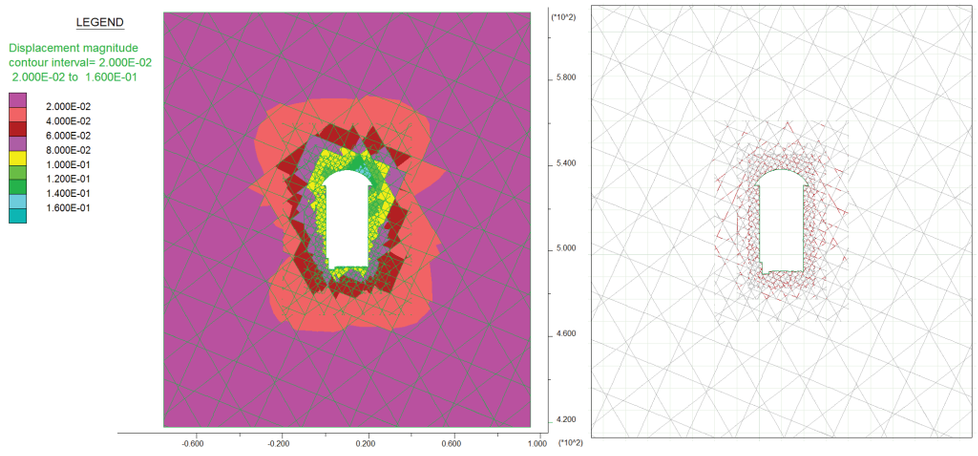

Fig. 10 - Total displacement (in m) around the machine hall. Total maximum displacement is around 15 cm. All the area around the cavern endures around or more than 10cm displacement (left). Open joints (in red) around the machine hall cavern after 100 000 cycles. Open joints reach distances as far as 20 m from the cavern walls (right)

8. DYNAMIC LOADING

8.1 Simulating the Wave

A dynamic analysis is somehow necessary here, considering the area where the powerhouse is built. According to the IS (Indian Standards) code, the area lies in zone IV, which means it is highly seismic and has endured several earthquakes in the last years. The numerical simulation of an earthquake is carried out by applying a dynamic loading to the model. The initial state is the nearly stabilized model presented previously. Boundary conditions are modified to viscous boundary (or free-field motion) so the seismic waves are not reflected on the sides of the models but absorbed as if they propagated through an infinite field. The acceleration time history of a real earthquake looks like a random signatures, with many cycles of motions and a wide spectrum of frequencies. In this study, since the objective is a general assessment of earthquake effect, the signal was simplified to a sinusoidal function. Based on literature and previous simulations carried out in the area (e.g. Pal et al., 2011), a shear sinusoidal wave of frequency 3 Hz was applied at the base of the model for 3 s, and let it propagate upwards. The peak ground acceleration is assumed to

be 1 m/s^2. In order to compensate for the viscous bottom boundary, the applied shear stress was doubled, giving a value of 0.26 MPa.

8.2 Earthquake Effects

Figure 11 presents the main results for the dynamic analysis, that is the total convergence at different elevation in the machine hall along time. Displacement at the crown are also shown and total displacement after 6 s. Results show that if the movement was limited to less than 20 cm under static conditions, it could largely excess one meter in case of an earthquake. Maximum displacement occurs during the first second of the earthquake. After it has stopped (t = 3 s), no further movement is observed. The most sensitive zone is at the bottom of the cavern, while the crown is a bit less affected. It seems that most of the displacement occurs on the upstream wall (right of the model) and that a large zone is mobilized (at least 6 m far from the cavern).

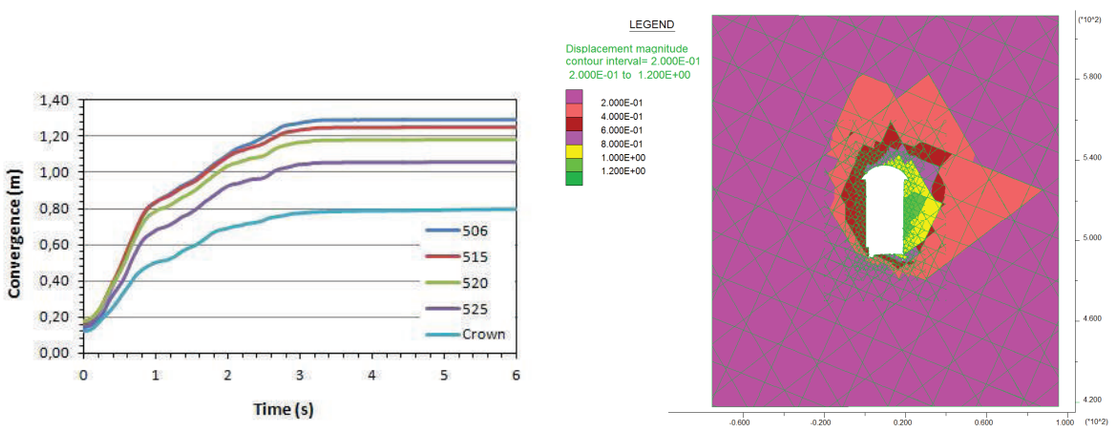

Fig. 11 - Simulated convergence and displacement for different elevations in the cavern and in the crown under a dynamic loading of 3 Hz (left; see text for details).
Total displacements after 6 s (right)

Additional simulations were carried out to analyze the effect of the frequency and the amplitude of the earthquake. Results are presented in Figure 12. They show that there is a critical frequency (at least 3 Hz) under which frequency variations have almost no effect on the displacement. To the contrary, above this value, the displacement increases rapidly with the frequency. The simulations indicate that the cavern stability is highly susceptible to dynamic loads.

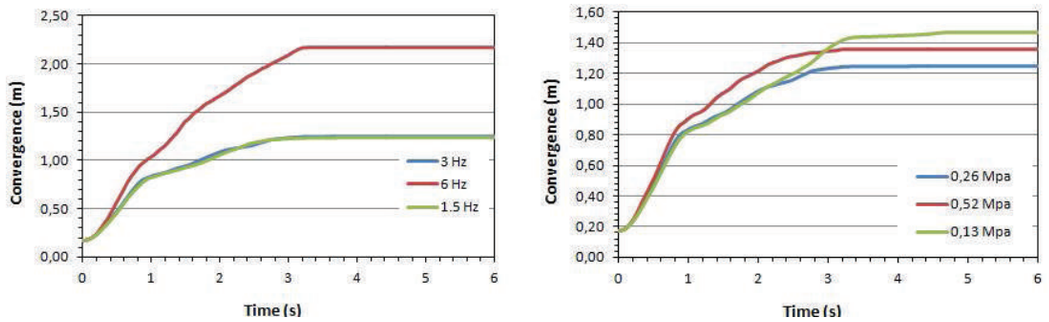

Fig. 12 - Simulated convergence at elevation 515 under a dynamic loading for various frequencies (left) and amplitudes (right)

9. CONCLUSIONS

Several underground structures have undergone severe damages during recent earthquake events. Numerical simulations indicate that the performance of underground structures can be adversely affected during earthquakes. A case study on the stability of a large cavern with earthquake loading is highlighted. In this cavern a certain number of instabilities were observed during and after construction in the Tala hydroelectric power house. The walls of the cavern are continuing to converge, at a slow rate, and approximately 5% of the bolts in the powerhouse are reported to have failed (and situation could be worse that it appears according to the simulations). Plans are underway to stabilize this important underground structure. Distinct element numerical simulations have confirmed what was observed in situ. Convergences have been fairly well reproduced and some information was obtained regarding bolts failures. Observations in the cavern show that the expulsed bolts were free of grouting, indicating that may be the reason of these failures (may be the not so good installation). Dynamic simulations have also shown that the cavern stability is highly susceptible to earthquake and especially sensitive to high frequencies, and that large displacements could occur under dynamic loading.

Based on this study, recommendations are being proposed to stabilize the walls of the cavern. Complementary 3D simulations are intended to be carried out to improve these results.

Acknowledgements

The authors would like to thank the organisations DGM (Mr. Dowchu Drukpa), DGPC (Mr. Yeshi Dorji) and CSMRS (Dr. Rajbal Singh) for their inputs. The Royal Norwegian Embassy is thanked for sponsoring the co-operation project between DGM and NGI.

References

Aydan, O., Ohta, Y., Genis, M., Tokashiki, N. and Ohkubo, K. (2010). Response and Stability of Underground Structures in Rock Mass during Earthquakes, Rock Mechanics and Rock Engineering. Vol. 43, pp. 857-875.

Barton, N. (1984). Effects of Rock Mass deformation on Tunnel Performance in Seismic Regions, Proc. Caracas Symp., Adv. Tunnel. Technol. and Subsurf. Use, Vol. 4, No. 3, pp. 89-99.

Barton, N. (1994) A Q-System Case Record of Cavern Design in Faulted Rock, 5th Int. Rock Mechanics and Rock Engineering Conf., Tunnelling in difficult conditions, Torino, Italy, pp. 16.1-16.14.

Barton, N., R. Lien and J. Lunde (1974). Engineering classification of rockmasses for the design of tunnel support, Rock Mechanics, Vol. 6, No. 4, pp. 189-236.

Bhasin, R., Abokhalil, M., Kaynia, A.M., Høeg, K., Paul, D.K. and Pal, S. (2010). Numerical simulations of earthquake effect in underground structures, Symposium on Earthquake Engineering, 14, Roorkee, India, pp. 1384-1394.

Bhasin, R. and Grimstad, E. (1996). The use of stress-strength relationships in the assessment of tunnel stability. Tunnelling and Underground Space Technology, Vol. 11 No. 1, pp. 93-98.

Bhasin, R. and Høeg, K. (1997). Numerical modelling of block size effects and influence of joint properties in multiply jointed rock, Tunnelling and Underground Space Technology, 22(3), pp. 407-415.

Bhasin, R. and Høeg, K. (1998). Parametric study for a large cavern in jointed rock using a distinct element model (UDEC-BB), Int. J. Rock Mech. Min. Sci., 35(1), pp. 17-29.

Bhasin, R., Kaynia, A.M., Paul, D.K., Singh, Y. and Pal, Shilpa. (2006). Seismic behaviour of rock support in tunnels. Proceedings 13th Symposium on Earthquake Engineering, Indian Institute of Technology, Roorkee, December 18-20.

Bhasin, R. and Pabst, T. (2013). Finite element and distinct element analysis of surrounding rock for an underground powerhouse in the Himalayas. International Symposium on Tunnelling and Underground Space Construction for Sustainable Development, March 18-20 Seoul, South Korea.

Goel, R.K., Singh, B. and Zhao, J. (2012). Underground Infrastructures - Planning, Design, and Construction, Elsevier publication, Printed in USA,p 335.

Grimstad, E., Bhasin, R., Hagen, A.W., Kaynia, A. and Kankes, K. (2003). Q-system advance for sprayed lining, Part 1-Tunnels and Tunneling International (T&T) January 2003 and Part II - (T&T) March 2003.

Hashash, Y.M.A., Hook, J.J. and Scmidt, B. (2001). Seismic design and analysis of underground structures, Tunnelling and Underground Space Technology, 16 (4), pp.247-293.

Heuze, F.E. and Morris, J.P. (2007). Insights into ground shock in jointed rocks and the response of structures there-in, International Journal of Rock Mechanics and Mining Sciences, 44(5), pp. 647-676.

Naik, S.R., Nair, R., Sudhakar, K., and Nawani, P.C. (2011b). Final report on back analysis using numerical modeling of powerhouse complex of Tala hydroelectric project, Bhutan, Report No. NM1003C, 42p.

Naik, S.R., Sudhakar, K., and Nair, R. (2011a). Final report on instrumentation, monitoring and data analysis at power complex, Tala hydro power plant, Bhutan, Report No. NM1001C/02, 54p.

Okamoto, S., Tamura, C., Kato, K. and Hamada, M. (1973). Behaviors of submerged tunnels during earthquakes, Proceedings of the Fifth World Conference on Earthquake Engineering, Vol. 1, Rome, Italy, pp.544-553.

Owen, G.N. and Scholl, R.E. (1981). Earthquake engineering of large underground structures, Report no. FHWA/RD-80/195, Federal Highway Administration and National Science Foundation, USA.

Pal, S., Kaynia, A.M., Bhasin, R. and Paul, D.K. (2009). Distinct element stability analysis of Surbhee resort landslide in Garhwal Himalayas, India, Proc. World Congress in Disaster Management, New Delhi.

Palmström A. (1995). RMi - a system for characterizing rock mass strength for use in rock engineering, Journal of Rock Mechanics and Tunnelling Technology, 1(2), pp. 69-108.

Sengupta, S., Subramanyam, D.S., Joseph, D., and Sinha, R.K. (2007). The role of National Institute of Rock Mechanics in-situ geotechnical investigations (1979 to 2002) at Tala hydroelectric project Bhutan, In Proceedings of Int. Workshop on Experiences Gained in Design and Construction of Tala Hydroelectric Project Bhutan, June 14-15, 2007, New Delhi, pp.150-172.

Sharma, B.N., Singh, R., Goyal, D.P., and Khanzanchi, R.N. (2004). Experience of Dywidag rock bolts in machine hall cavern at Tala project, Journal of New Building Materials & Construction World, 9(11), pp. 68-74.

Singh, B., Jethwa, J.C., Dube, A.K. and Singh, B (1992). Correlation between observed support pressure and rock mass quality, Tunnelling and Underground Space Technology, Vol. 7, No. 1, pp. 59-74.

Singh, R. (2005). Instrumentation at Tala hydroelectric project in Bhutan, In Training Course on Geotechnical Instrumentation for River Valley Projects, New Delhi, February 28 - March 9, pp. 42-66.

Singh, R., Chowdhry, A.K., Sharma, R.N., Goyal, D.P. and Khazanchi, R.N. (2002). Wall support system for powerhouse cavern of Tala Hydroelectric Project in Bhutan Himalayas, In Proceedings of Indian Rock Conference, 28-29 Nov. 2002, New Delhi, pp. 132-142.

Singh, R. and Goyal, D.P. (2005). Compendium of published papers on 1020 MW Tala hydroelectric project, Published by Tala Hydroelectric Project Authority, Gedu, Bhutan.

Singh, R. and Sthapak, A.K. (2007). Proceedings International workshop on experiences gained from the design and construction of Tala hydro-electric project, Bhutan, Organised by ISRMTT, CSMRS, THAPGB, New Delhi, 2007

Sripad, Rao, R.V., Gupta, R.N., Sudhakar, K., Raju, G.D., Singh, R. and Sharma, B.N. (2003). Instrumentation to study rock mass behaviour of machine hall cavern at Tala hydroelectric project, Bhutan, Proceedings of the International Conference on Accelerated Construction of Hydropower Projects, Gedu, Bhutan, October 15-17, I: VII 1-12.

Rao, V. R., Alagh, P.K., Chowdhry, A.K., Sharma, B.N., and Theraja, D.V. (2003a). Evaluation of rock bolt failure mechanism in Tala HE project, Bhutan, Proceedings of the International Conference on Accelerated Construction of Hydropower Projects, Gedu, Bhutan, October 15-17, II: V 30-37.

Rao, V.R., Gupta, R.N., Raju, G.D., Chowdhry, A.K., Chug, I.K., and Alagh, P.K. (2003b). Performance of rigid support system in cross openings around major caverns, Proceedings of the International Conference on Accelerated Construction of Hydropower Projects, Gedu, Bhutan, October 15-17, II: V 38-46.

Rao, V.R., Raju, G.D. and Chowdhry, A.K. (2007). Stress analysis of desilting chamber complex of Tala hydroelectric project, Proceedings of the International Workshop on Experiences Gained in Design and Construction of Tala Hydroelectric Project Bhutan, June 14-15, New Delhi, pp.283-297.

Wang, J.N. (1993). Seismic design of tunnels: A state-of-the-art approach, monograph 7, Parsons, Brinckerhoff, Quade and Douglas Inc, New York.

WAPCOS (2011). Draft report of DGPC, Tala Hydroelectric project, on additional rock bolt installation for strengthening of power-house caverns, 43p.